IUST Iran University of Science and Technology

Iranian Journal of Electrical and Electronic Engineering

Journal Homepage: ijeee.iust.ac.ir

Research Paper

Deep Learning-Based Ultrasound Image Despeckling by Noise Model Estimation

O. Mahmoudi Mehr*, M. R. Mohammadi*, and M. Soryani*(C.A.)

Abstract: Speckle noise is an inherent artifact appearing in medical images that significantly lowers the quality and accuracy of diagnosis and treatment. Therefore, speckle reduction is considered as an essential step before processing and analyzing the ultrasound images. In this paper, we propose an ultrasound speckle reduction method based on speckle noise model estimation using a deep learning architecture called "speckle noise-based inception convolutional denoising neural network" (SNICDNN). Regarding the complicated nature of speckle noise, an inception module is added to the first layer to boost the power of feature extraction. Reconstruction of the despeckled image is performed by introducing a mathematical method based on solving a quadratic equation and applying an image-based inception convolutional denoising autoencoder (IICDAE). The results of various quantitative and qualitative evaluations on real ultrasound images demonstrate that SNICDNN outperforms the state-of-the-art methods for ultrasound despeckling. SNICDNN achieves 0.4579 dB and 0.0100 additional gains on average for PSNR and SSIM, respectively, compared to other methods. Denoising ultrasound based on its noise model estimation is not only a novel approach in comparison to traditional denoising autoencoder models but also due to the fact that it uses mathematical solutions to recover denoised images, SNICDNN shows a greater power in ultrasound despeckling.

Keywords: Denoising Autoencoder, Inception Convolutional Neural Network, Speckle Noise Estimation, Ultrasound Image Denoising.

1 Introduction

ULTRASOUND imaging plays a vital role in medicine. It is widely used to view internal anatomy, including the abdomen, breast, liver, kidney, tendons, muscles, joints, and vessels, to discover potential lesions or pathology needs.

Iranian Journal of Electrical and Electronic Engineering, 2023.
Paper first received 30 Apr 2022, revised 07 May 2023, and accepted 21 May 2023.
*The authors are with School of Computer Engineering, Iran University of Science and Technology, Tehran, Iran.
E-mails: omid_mahmoudimehr@alumni.iust.ac.ir, mrmohammadi@iust.ac.ir, and soryani@iust.ac.ir.
Corresponding Author: M. Soryani.
https://doi.org/10.22068/IJEEE.19.3.2506.

This imaging modality offers several advantages over other medical diagnosis methods, such as being economical, efficient, non-invasive, real-time, and, more importantly, free of harmful radiation. Its safety considerably matters when observing pregnant women [1, 2].

Unfortunately, owing to the nature of the acquisition system, ultrasound images are contaminated by speckle noise. Speckle is a random deterministic interference that significantly degrades the contrast and textural features and adversely affects diagnosis and treatment [3].

Hence, not only does it affect human interpretation, but also it reduces the accuracy of various post-processing tasks such as feature extraction, segmentation, registration, and classification [4, 5]. Thus, speckle reduction is a crucial step before the processing and analysis of

ultrasound images in order to obtain reliable and accurate results. Therefore, many researchers have focused on this issue, and various methods of ultrasound image denoising have been proposed in the literature. These methods can be classified into two branches: conventional and deep-learning-based denoisers.

Lee [6], the non-local mean (NLM) [7], Wiener [8], the speckle reducing anisotropic diffusion (SRAD) [9], and classical bilateral filters (CBF) [10] may be mentioned as the most commonly used conventional denoising techniques. Filtering is a set of operations in which the image is convolved with a smoothing function in the spatial domain. Indeed, the filtering of signals is regarded as a fundamental algorithm in basic image processing and has long been used for smoothing, sharpening, edge detection, and contrast enhancement [11]. Lee and Wiener filters are adaptive filters based on local statistics of the noisy signal [12]. The major drawback of adaptive filters is their tendency to blur images, leading to unsatisfactory denoised results [2]. SRAD is an iterative method that tries to preserve the edges while reducing the noise [9].

Nonetheless, meaningful structural details are removed, and artifacts are produced [1, 3]. NLM filter reduces the noise by utilizing the repetitious information present in the noisy signal. In other words, each pixel of the denoised image is reconstructed by a weighted average of all values in a noisy image, but unfortunately, NLM fails to keep edges or delicate structures [1, 13]. CBF filter replaces the central image pixel value with a weighted average of its neighbors, where the weight computation is dependent on both spatial and intensity distances. In conclusion, due to the spatial processing nature of these methods, they often fail to preserve features such as edges and produce artifacts in the denoised image [14, 15].

Lately, deep learning has outperformed other methods in various research fields, especially in image analysis and computer vision [16]. Deep learning algorithms are based on learning to extract optimal features from raw data, which has traditionally been done by conventional methods [17]. Convolutional neural networks (CNNs) are the most popular deep architectures that include several modules, such as convolutional layers, rectified linear unit (ReLU) [18], and batch normalization [19]. The main role of the convolutional layer is to perform different convolution operations on the input image so that local features at different positions and scales are detected [16]. However, to the best of our knowledge, although there have been many attempts in the literature to denoise images, ultrasound despeckling methods based on deep learning have not been sufficiently discussed. Lee et al. (2018) [20] applied convolutional denoising autoencoder (CDAE) to Gaussian image denoising, resulting in performance superiority over conventional methods. Feng et al. [21] designed US-Net architecture to reduce the ultrasound speckle noise by defining a new loss function. Their advanced technique was shown to be able to compete with filtering techniques. Zhang et al. [22] proposed a DnCNN, named residual learning, to remove Gaussian noise. In this approach, a noise model was predicted from noisy input, and the denoised image was then reconstructed by subtracting the noise model from the noisy image. Zhang et al. [23] applied the same principle as DnCNN, in which a dilated residual network tries to learn the difference between noisy input and the actual image.

As shown by He et al. [24], when the noisy observation is much more like the clean image than the noise model, the residual mapping will be easier to optimize. Motivated by [22], we developed an innovative method, SNICDNN, to reduce the ultrasound speckle noise by using the noise model. SNICDNN is a modified version of DnCNN to which the inception module is added to boost the power of feature extraction [25]. Our experiments show that the speckle noise definition meets the prerequisite claimed by [24]. Thus, we apply SNICDNN to predict the speckle noise model.

Nevertheless, reconstructing a denoised image from speckled observation is not as straightforward as reconstructing a Gaussian noisy image. To resolve this, we devised an IICDAE assisted mathematical solution to obtain the denoised image. Finally, the performance of our method is comprehensively compared with other state-of-the-art denoising methods.

The main contributions of our proposed method are as follows:

i) Ultrasound speckle noise reduction based on its noise model estimation.
ii) Introducing and solving a mathematical equation based on the speckle noise model to achieve the despeckled image.
iii) Proposing a solution to handle the limited dataset for ultrasound images used in training.

The reminder of the paper is organized as follows: In Section 2, we present the speckle noise model formulation. Section 3 describes our method for ultrasound image denoising based on the speckle noise model. In Section 4, we provide experimental results on real ultrasound images. Finally, we conclude our work in Section 5.

2 Speckle Noise Model

The most critical part of developing a method for recovering a signal from its noisy observation is to opt for a reasonable definition of the speckle noise, which can acceptably represent the noise formation process. In ultrasound imaging, a universally agreed definition of such a model still seems to be lacking, but several possible formulations whose feasibility and practicality are confirmed exist [26]. Based on the experimental measurements from the signal processing stages occurring inside a scanner, including logarithmic compression, low-pass filtering, interpolation, and scan conversion, Loupas et al. [27] have shown that the observed noisy speckled signal can be modeled as follows:

$$y = \sqrt{x}n + x \quad (1)$$

Where x denotes the actual signal and n is a zero-mean Gaussian noise. It has been shown that the mentioned definition fits the data better than the multiplicative model or Rayleigh model. It has also been used successfully in many studies [28-30].

To better understand the nature of the noise model, we show what was depicted by [31]. Figure 1 shows a synthetic 1D signal corrupted by speckle and additive Gaussian noise with σ=5. This figure indicates that the appearance of speckle noise is more substantial than additive Gaussian noise. Therefore, it is necessary to recover the true signal before sending it to display [32].

3 Materials and Methods

In this section, we present the details of our proposed SNICDNN architecture for ultrasound despeckling. We mainly seek to recover the actual signal by learning to map a speckled observation to a speckle noise model using SNICDNN. In other words, the output of the SNICDNN represents the predicted speckle noise. Then, the despeckled signal is obtained by solving a quadratic equation derived by Eq. (1) for given y and predicted speckle noise $\hat{n}$. To perform this, the following two steps are taken:

i) Training the convolutional neural network with an Inception module.
ii) Denoised image reconstruction, given the estimated noise model and the noisy input.

3.1 Intuition

Before proceeding with the method, it is worth mentioning the intuition of learning speckle noise instead of using the actual signal, which is done by denoising autoencoders [33]. The reasons that we have found it promising are twofold. First, regarding Eq. (1), we notice a nonlinear equation with two variables. It can be intuitively understood that learning speckle noise would be easier for the convolutional neural network since there is a single noise variable in Eq. (1). On the other hand, choosing the traditional learning policy used by denoising autoencoders seems trickier because there are two variables of the actual signal with different exponents. Second, as He et al. [24] mentioned, learning the noise model is preferable when encountering identity mapping.

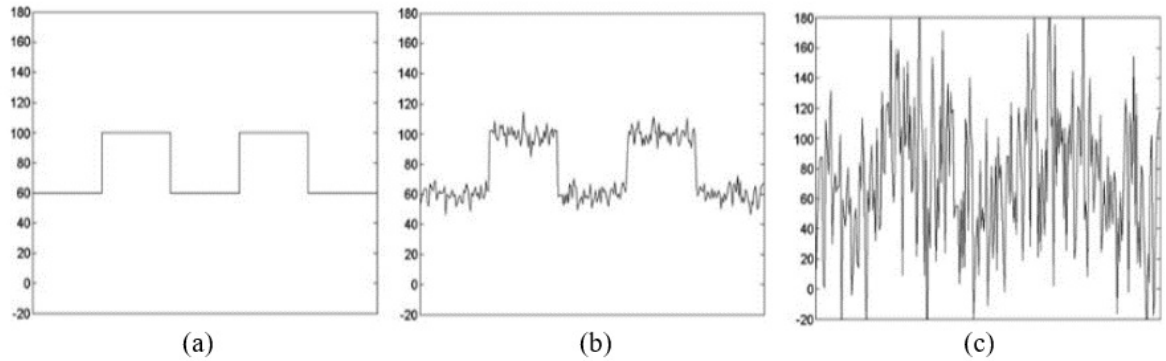

Fig. 1 Illustration of two physical noise models in one dimension [31]. (a) Noise-free 1D signal. (b) Signal contaminated by additive Gaussian noise with σ=5. (c) Signal contaminated by speckle noise with σ=5.

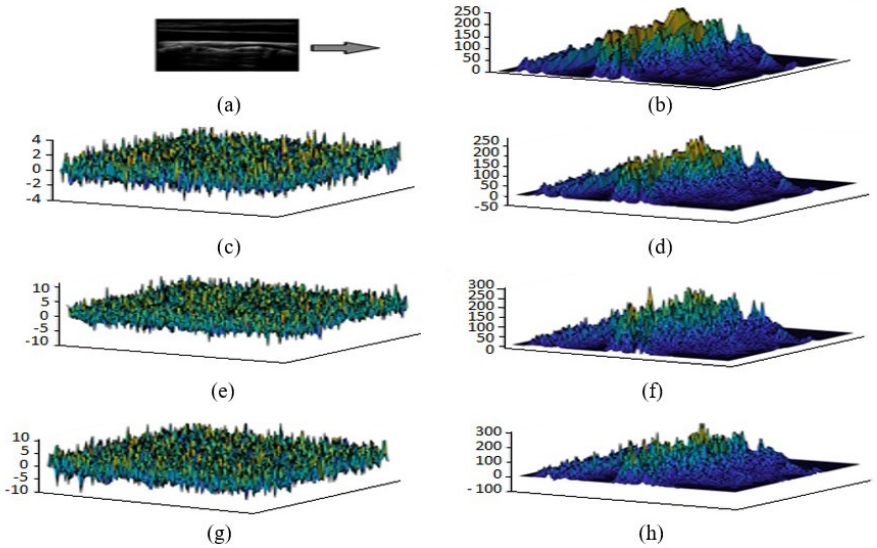

Fig. 2 Comparisons between actual and speckled signal with different noise variances. (a) An ultrasound image. (b) The ultrasound signal representation. (c) Noise with σ^2=1. (d) Speckled signal with σ^2=1. (e) Noise with σ^2=4. (f) Speckled signal with σ^2=4. (g) Noise with σ^2=8. (h) Speckled signal with σ^2=8.

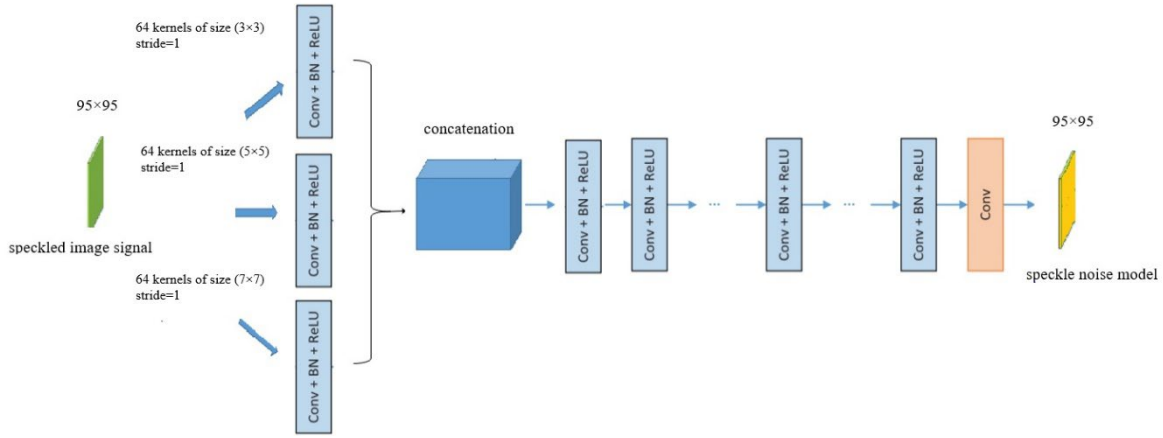

Fig. 3 The architecture of the proposed SNICDNN.

To illustrate this, an ultrasound image is used and contaminated with three different noise variances, including 1, 4, and 8, as shown in Fig. 2. This figure reveals that the speckled signals look more like the actual signals than their corresponding noise signals. Therefore, we conclude that using the proposed method, speckle reduction can be more efficiently and effectively addressed.

3.2 Network Architecture

Training a deep CNN for a specific task generally involves two steps: network architecture design and model learning from training data. For the CNN architecture, DnCNN [22] is modified by exploiting an inception module to extract the optimum local features with different kernel sizes to boost the overall performance [25]. Furthermore, since the speckle noise is a random phenomenon, looking at the input on different scales gives us a more accurate insight into the noise distribution. The proposed SNICDNN is shown in Fig. 3. For the first layer, the inception module consists of three convolutional layers with different kernel sizes of 3×3, 5×5, and 7×7, followed by batch normalization and ReLU, utilized for nonlinearity, producing 64 feature maps separately. The middle layers are also the same, except for the kernel size, which is only 3×3. A convolutional kernel with a size 3×3 is used for the last layer to estimate the speckle noise. To ensure that each feature map of the layers has the same size as the input, zeros are padded before convolution. In summary, SNICDNN aims to learn a mapping function $R(yi) \approx n$ using noisy signal and noise model

observations as the training data. Since we try to minimize the difference between predicted noise and actual noise, we use the mean square error loss function defined as follows:

$$L_{MSE} = \frac{1}{2N}\sum_{i=1}^{N}\|R(y_i) - n_i\|^2 \quad (2)$$

3.3 Denoised Image Reconstruction

The previous sections described how to estimate the speckle noise. The denoised image should be approximated based on the estimated speckle noise model and given a noisy signal. However, since Eq. (1) is much more complicated than the additive Gaussian noise equation and the despeckled signal reconstruction is not easy, a method based on solving a quadratic equation deriving from Eq. (1) is proposed here. After simplifying Eq. (1), it can be rewritten in quadratic form:

$$\hat{x}^2 - (2y + \hat{n}^2)\hat{x} + y^2 = 0 \quad (3)$$

Where $\hat{x}$ denotes the denoised variable of different pixels in an image that should be derived. The delta rule is the most popular approach for solving a quadratic equation. Regarding Eq. (3), the delta rule can be formulated as:

$$\Delta = (-(2y + \hat{n}^2))^2 - 4y^2 \quad (4)$$

In general, there are three possible conditions for the nature and number of roots, depending on the delta value.

- **Case 1:** $\Delta > 0$

When delta is bigger than zero, there are two distinct real roots. This case occurs when the following criterion is met:

$$\Delta > 0 \rightarrow \hat{n}^2 > -4y \quad (5)$$

The two real roots are derived through the following formula:

$$\hat{x}_1, \hat{x}_2 = \frac{(2y + \hat{n}^2) \pm \sqrt{\Delta}}{2} \quad (6)$$

Equation (6) shows that there are two different denoised values for the discussed location, while one value should be recovered for each pixel to gain a denoised image. In this case, an appropriate root should be chosen. The IICDAE network is proposed as a referee to assess the quality of roots in this study. It is important to keep in mind that the quality of the results depends on the referee's accuracy. As shown in Fig. 4, IICDAE is a convolutional denoising autoencoder [20] modified by adding an inception module to the first layer of the encoding phase to boost the power of feature extraction. Choosing the best root is quite simple. Overall, the speckled noisy signal is fed into both SNICDNN and the referee architecture. When case (1) is satisfied, for every noisy signal location, two roots are given to the referee for assessing and choosing the best root with a straightforward algorithm in which the best root has the closest absolute distance to what IICDAE predicts. A straightforward way to reduce the reference rate to the referee is to substitute the roots in Eq. (1) and evaluate which root holds for the equation. It is worth mentioning that wherever the value of the noisy signal is greater than zero, case (1) takes place.

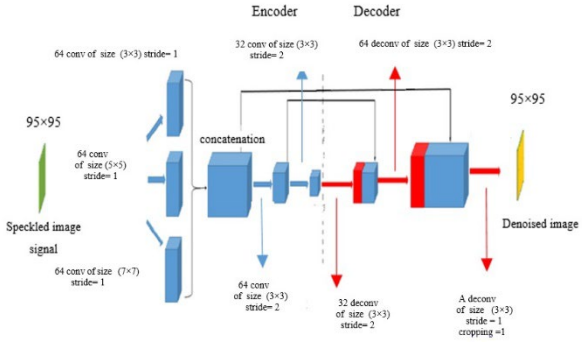

Fig. 4 Referee architecture for denoised reconstruction.

- **Case 2:** $\Delta = 0$

When delta is zero, then there is precisely one repeated root. Case (2) occurs when the following condition is met:

$$\Delta = 0 \rightarrow \hat{n}^2 = -4y \quad (7)$$

The reconstructed pixel is calculated as:

$$\hat{x} = \frac{(2y + \hat{n}^2)}{2} \quad (8)$$

In case (2), there is no need to assess pixels. Moreover, negative noisy signal value is the necessary condition for case (2) to happen.

- **Case 3:** $\Delta < 0$

The biggest challenge is when the delta is less than zero, which results in two complex roots. That is:

$$\Delta < 0 \rightarrow \hat{n}^2 < -4y \rightarrow -\sqrt{-4y} < \hat{n} < \sqrt{-4y} \quad (8)$$

It is well known that complex values in an image context are unacceptable. The magnitude of the derived numbers (which is the same for both complex roots) is calculated to eliminate the complex values.

To sum up, the fundamental steps needed to denoise a speckled signal are shown as a flowchart in Fig. 5.

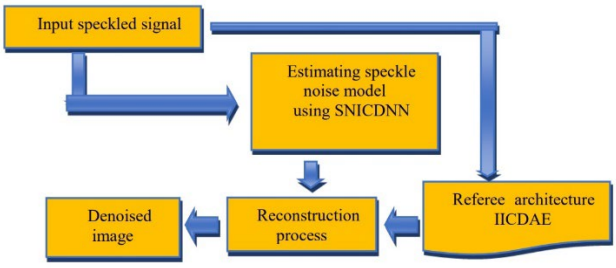

Fig. 5 General flowchart of our proposed despeckling method.

4 Results

4.1 Dataset

Deep learning methods require large datasets to be trained well. This can be a severe problem in the case of medical images, such as ultrasound, for which limited datasets are available [34]. To deal with the mentioned issue, we have used two datasets for training. The first dataset is named STL-10 proposed in [35], including 10000 gray-level non-medical images. The second includes 84 ultrasound images of the common carotid artery (CCA) (mentioned in [36]). For training, both STL-10 and authentic ultrasound images are used. One hundred sixty-eight images are obtained from 24 images of CCA through augmentation and added to STL-10 for training. The rest of the CCA images (i.e., 60 images) are set up for two phases: 20 images are augmented to 160 images for validation in the training process, and 40 images are used for the testing phase. All learning-based methods, including the present one, share the same training dataset.

It is essential that the training data be contaminated with speckle noise, according to Eq. (1). In this regard, blind denoising [22] is used, in which images are contaminated with random noise with variances in the discrete range of 1 to 6.

4.2 Parameter Setting and Network Training

To train the proposed methods (SNICDNN and IICDAE), the adaptive moment estimation (ADAM) optimizer with default hyper-parameters recommended by [37] is employed. SNICDNN and IICDAE are initialized with the same mini-batch size of 20 and trained for 60 and 150 epochs, respectively. Figure 6 shows the training and validation curves for these networks.

All experiments were carried out in MATLAB R2018b using a deep learning toolbox running on an Intel ® Core™ i7-8550U 1.80GHz CPU and an NVIDIA GeForce 940MX GPU.

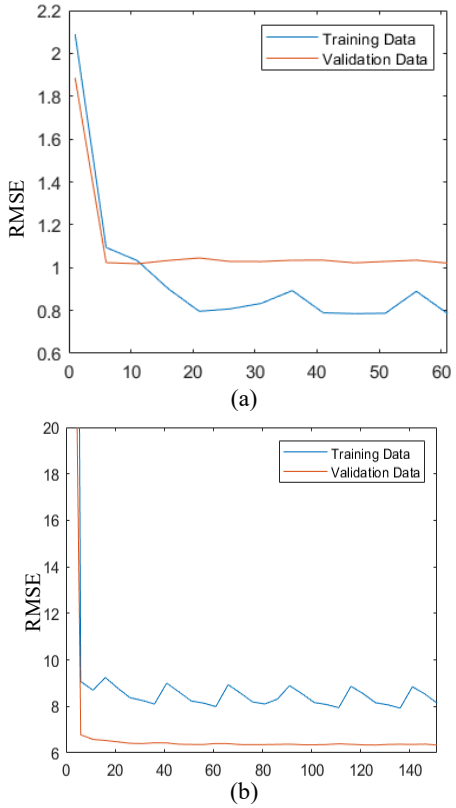

Fig. 6 RMSE according to epoch number. (a) SNICDNN. (b) IICDAE.

4.3 Comparison of the Methods

In this section, the proposed SNICDNN is compared with several state-of-the-art denoising methods, including four conventional methods, i.e., Lee [6], NLM [7], Wiener [8], SRAD [9], and CBF [10], besides four deep-learning-based methods, i.e., CDAE [20], US-Net [21], DRN [23] ,and image-based SNICDNN. The latter has the same architecture as SNICDNN, but it uses a different training policy, attempting to learn a denoised

image from a noisy signal with the MSE loss function. This evaluation aims to show the superiority of SNICDNN over its corresponding architecture with the typical training policy adopted in autoencoders. For all the compared methods, hyperparameters are set as suggested in their corresponding papers.

5 Discussion

To evaluate the capability of the proposed method, we conduct experiments on 40 test images contaminated with four different noise variances ($\sigma 2$ = 2, 4, 6, and 8). The quantitative performance of denoising methods is calculated through peak signal-to-noise ratio (PSNR) [38] and structural similarity index (SSIM) [39]. The average and standard deviation of PSNR and SSIM of denoising methods are summarized in Tables 1 and 2 forcomparison. The best results are represented in bold. Different noise levels. This table shows that SNICDNN achieved the best PSNR results at all noise variances. As an illustration, SNICDNN achieved 0.4597 dB and 0.1736 dB gains (on average) compared to the methods of DRN and our referee, respectively. The significant difference between SNICDNN and image-based SNICDNN indicates that learning the speckle noise model instead of the clean image can lead to a better speckle noise reduction.

Table 2 compares different methods in terms of average SSIM. It is shown that SNICDNN ranks first and achieves 0.0100 and 0.0029 gains compared to CDAE and IICDAE, respectively.

Figure 7 presents the average PSNR of different methods for all noise variances, where the color bar indicates the average SSIM. It is observed that SNICDNN has the highest value in terms of quality metrics. However, the high number of trainable parameters does not cause our proposed method to over-fit. It is worth noting that to learn the complicated nature of speckle noise, such a considerable number of parameters is a necessity.

To illustrate the effectiveness of the proposed method visually, its speckle reduction capability is examined on two authentic ultrasound images. Figs. 8-11 depict the visual results of the different methods for two noise variances. It is conspicuous that the Wiener filter, NLM filter, and SRAD retain much noise, while the Lee filter and US-net tend to produce over-smooth edges and textures. The image-based SNICDNN produces additional artifacts. On the other hand, SNICDNN and its referee (IICDAE) not only reduced the speckle noise, but also recovered sharp edges and fine details. Both quantitative and qualitative experiments demonstrate the feasibility of training a blind model of SNICDNN for speckle reduction of ultrasound images within a wide range of noise variances.

6 Conclusion

This study proposed a deep convolutional neural network for ultrasound image denoising based on speckle noise model prediction. In order to obtain the most accurate noise model estimation, we integrated the inception module and batch normalization into a convolutional neural network for better feature extraction and to speed up the training process, respectively. Reconstruction of the despeckled image was carried out by solving a quadratic equation for the given predicted speckle noise and noisy image. In the reconstruction process, IICDAE was employed as a referee network during the assessment. Extensive experimental results confirmed that the proposed method produced favorable despeckled images both quantitatively and qualitatively. Furthermore, the capacity of the proposed method to handle unknown noise variances was verified.

Intellectual Property

The authors confirm that they have given due consideration to the protection of intellectual property associated with this work and that there are no impediments to publication, including the timing to publication, with respect to intellectual property.

Funding

No funding was received for this work

Credit Authorship Contribution Statement

O. Mahmoudi Mehr: Idea & Conceptualization, Research & Investigation, Software & Simulation. **M. R. Mohammadi:** Idea & Conceptualization, Verification, Revise & Editing. **M. Soryani:** Idea & Conceptualization, Supervision, Revise & Editing.

Declaration of Competing Interest

The authors hereby confirm that the submitted manuscript is an original work and has not been

published so far, is not under consideration for publication by any other journal and will not be submitted to any other journal until the decision will be made by this journal. All authors have approved the manuscript and agree with its submission to "Iranian Journal of Electrical and Electronic Engineering".

Table 1 Average and standard deviation of PSNR results for different methods.

	Noise variance			
	2	4	6	8
Speckled signal	30.7496	27.8211	26.0941	24.9217
Lee [6]	29.4172±1.9905	29.068±1.9691	28.7325±1.9328	28.411±1.8829
NLM [7]	31.2135±1.4761	28.5514±1.3819	26.9991±1.3629	25.9448±1.2726
Wiener [8]	31.8959±1.8170	30.1953±1.6218	28.8847±1.5272	27.8905±1.4125
SRAD [9]	30.7391±1.6389	27.8637±1.6737	26.1984±1.7108	25.0949±1.6920
CBF [10]	29.8882±1.1292	27.6686±1.4083	26.1937±1.5521	25.119±1.5862
CDAE [20]	34.6846±1.7273	32.8564±1.7390	31.6431±1.7270	30.6887±1.6425
US-Net [21]	31.0951±0.6872	30.2614±0.8440	29.5245±0.9823	28.9374±1.0100
DRN [23]	34.6519±1.6686	32.8444±1.7130	31.7665±1.7126	30.9225±1.6527
IICDAE	34.9044±1.7371	33.1113±1.7797	32.0792±1.7577	31.235±1.6801
SNICDNN(image-based)	33.7651±1.5083	32.2637±1.5609	31.303±1.5859	30.5096±1.5146
SNICDNN	35.0885±1.7235	33.2362±1.7968	32.1991±1.7788	31.5006±1.7279

Table 2 Average and standard deviation of SSIM results for different methods

	Noise variance			
	2	4	6	8
Speckled signal	0.9095	0.8475	0.7959	0.7565
Lee [6]	0.8920±0.0244	0.8812±0.0260	0.8698±0.0291	0.8596±0.0303
NLM [7]	0.9238±0.0152	0.8839±0.0199	0.8536±0.0237	0.8299±0.0250
Wiener [8]	0.9220±0.0199	0.9034±0.0215	0.8839±0.0248	0.8663±0.0259
SRAD [9]	0.9099±0.0234	0.8479±0.0367	0.8000±0.0454	0.7623±0.0513
CBF [10]	0.8227±0.0374	0.7848±0.0305	0.7527±0.0290	0.7258±0.0316
CDAE [20]	0.9559±0.0107	0.9367±0.0147	0.9204±0.0176	0.9057±0.0192
US-Net [21]	0.7705±0.1005	0.7564±0.0968	0.7423±0.0930	0.7298±0.0901
DRN	0.9538±0.0093	0.9333±0.0135	0.9170±0.0162	0.9034±0.0171
IICDAE	0.9599±0.0105	0.9418±0.0147	0.9286±0.0171	0.9169±0.0185
SNICDNN(image -based)	0.9338±0.0114	0.9172±0.0145	0.9027±0.0171	0.8902±0.0190
SNICDNN	0.9624±0.0097	0.9444±0.0144	0.9307±0.0177	0.9214±0.0190

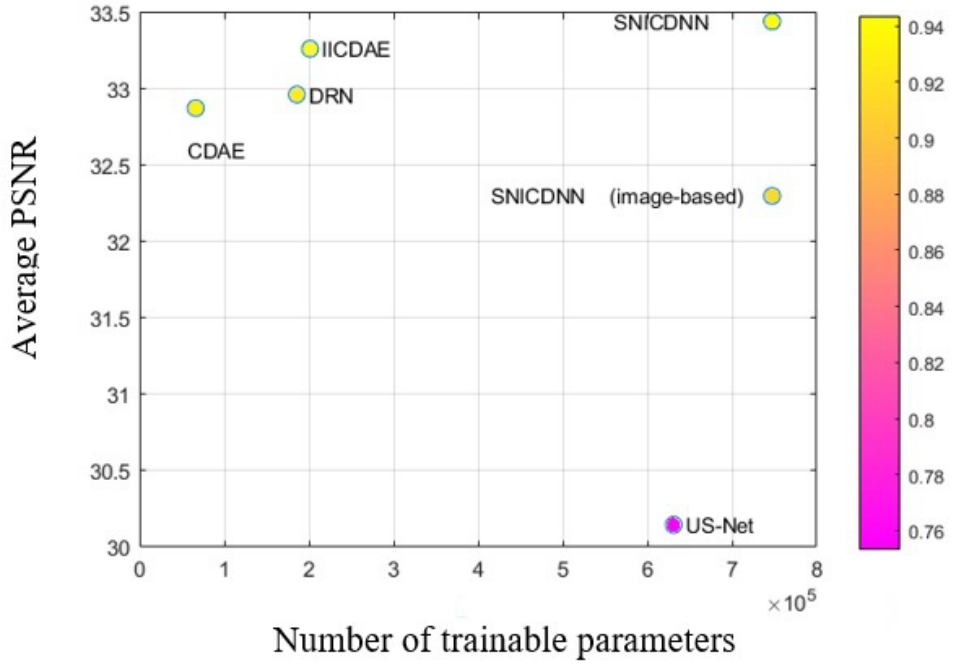

Fig. 7 PSNR, SSIM vs complexity.

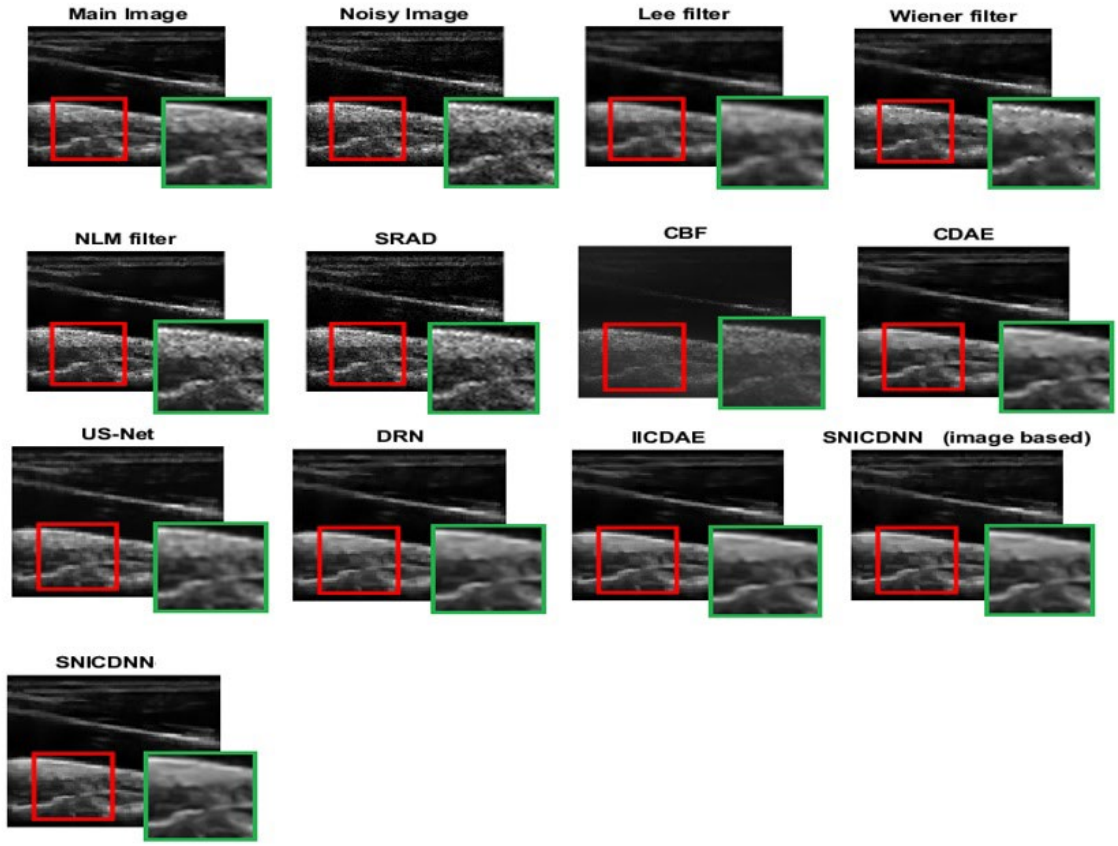

Fig. 8 Visual comparison of different methods for ultrasound image Ⅰ speckled with σ^2=4.

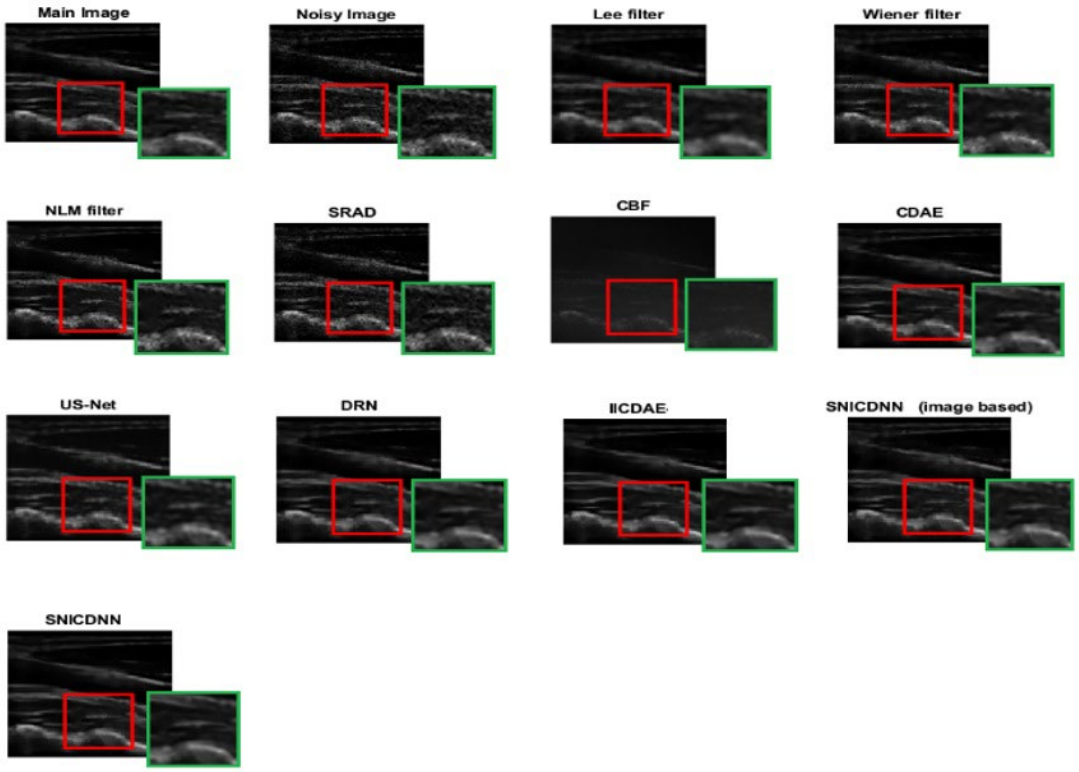

Fig. 9 Visual comparison of different methods for ultrasound image Ⅱ speckled with σ^2=4.

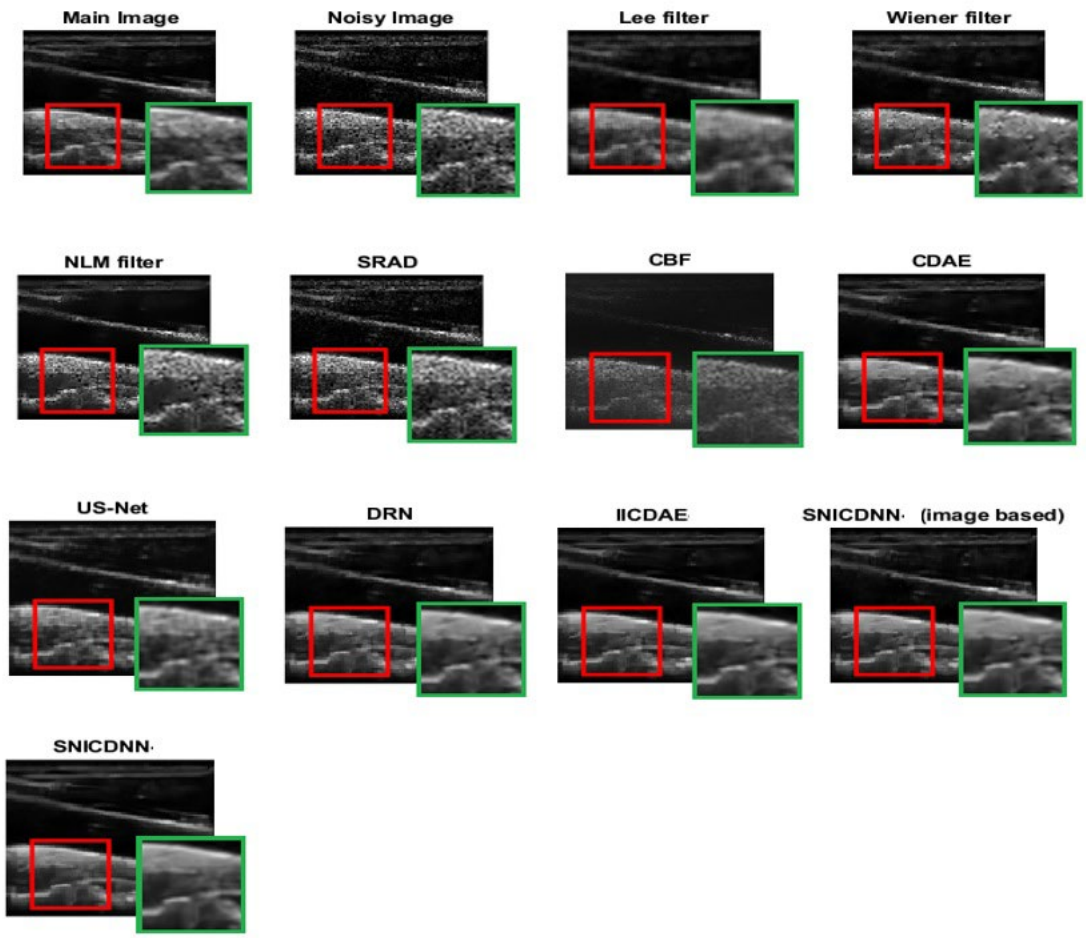

Fig. 10 Visual comparison of different methods for ultrasound image Ⅰ speckled with σ^2=8.

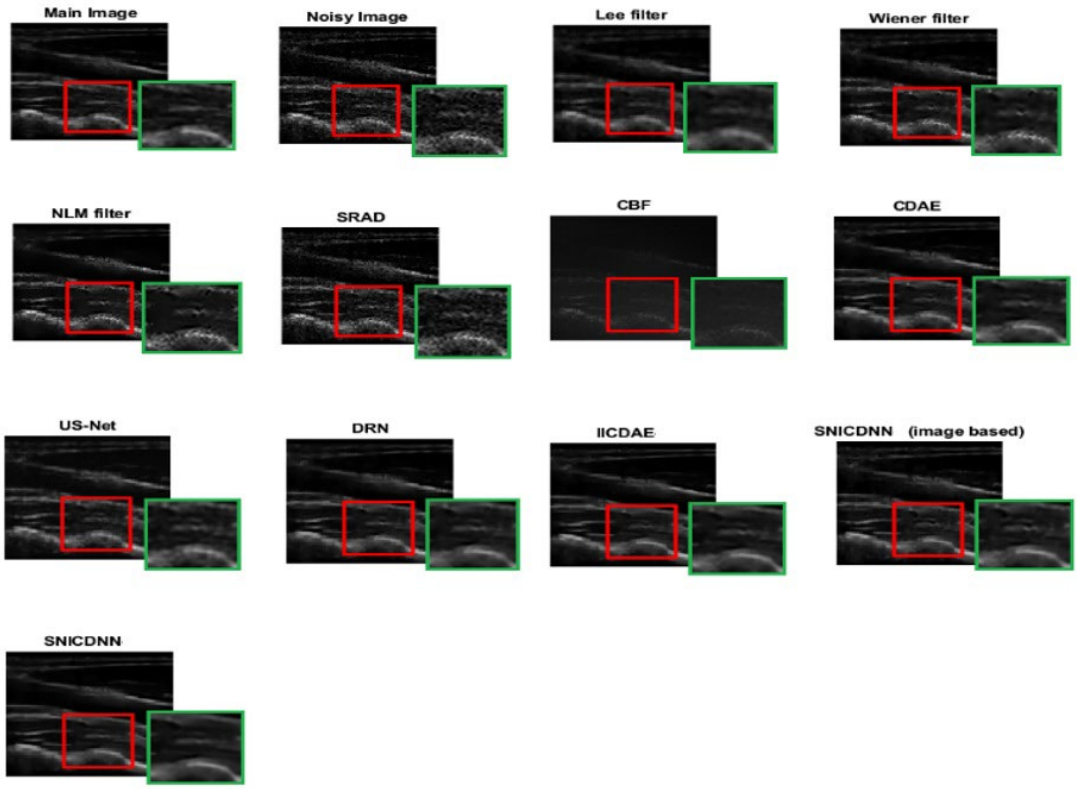

Fig. 11 Visual comparison of different methods for ultrasound image Ⅱ speckled with σ^2=8.

References

[1] J. Yang, J. Fan, D. Ai, X. Wang, Y. Zheng, S. Tang, and Y. Wang, "Local statistics and non-local mean filter for speckle noise reduction in medical ultrasound," *Neurocomputing*, Vol. 195, pp. 88-95, 2016.

[2] J. Zhang, G. Lin, L. Wu, and Y. Cheng, "Speckle filtering of medical ultrasonic images using wavelet and guided filter," *Ultrasonics*, Vol. 65, pp. 177-193, 2016.

[3] L. Zhu, W. Wang, J. Qin, K.H. Wong, K.S. Choi, and P.A. Heng, "Fast feature-preserving speckle reduction for ultrasound images via phase congruency," *Signal Processing*, Vol. 134, pp. 275-284, 2017.

[4] H. R. Shahdoosti and Z. Rahemi, "A maximum likelihood filter using non-local information for despeckling of ultrasound images," *Machine Vision and Applications*, Vol. 29, No. 4, pp. 689-702, 2018.

[5] S. Bonny, Y.J. Chanu, and K.M. Singh, "Speckle reduction of ultrasound medical images using Bhattacharyya distance in modified non-local mean filter," *Signal, Image and Video Processing*, Vol. 13, No. 2, pp. 299-305, 2019.

[6] J. S. Lee, "Speckle analysis and smoothing of synthetic aperture radar images," *Computer Graphics and Image Processing*, Vol. 17, No. 1, pp. 24-32, 1981.

[7] A. Buades, B. Coll, and J. M. Morel, "A review of Image Denoising Algorithms, with a New One," *Multiscale Modeling & Simulation*, Vol. 4, No. 2, pp. 490-530, 2005.

[8] J. S. Lim, *Two-Dimensional Signal and Image Processing*. Englewood Cliffs, New Jersey, USA, 1990.

[9] Y. Yu and S.T. Acton, "Speckle Reducing Anisotropic Diffusion," *IEEE Transactions on Image Processing*, Vol. 11, No. 11, pp. 1260-1270, 2002.

[10] K. Singh, S.K. Ranade, and C. Singh, "A hybrid algorithm for speckle noise reduction of ultrasound images," *Computer Methods and Programs in Biomedicine*, Vol. 148, pp. 55-69, 2017.

[11] B. Goyal, A. Dogra, S. Agrawal, B. S. Sohi, and A. Sharma, "Image denoising review: From classical to state-of-the-art approaches," *Information Fusion*, Vol. 55, pp. 220-244, 2020.

[12] J. Zhang, C. Wang, and Y. Cheng, "Comparison of Despeckle Filters for Breast Ultrasound Images," *Circuits, Systems, and Signal Processing*, Vol. 34, No. 1, pp. 185-208, 2015.

[13] S. Khare and P. Kaushik, "Efficient and robust similarity measure for denoising ultrasound images in non-local framework," *Journal of Intelligent & Fuzzy Systems*, Vol. 37, No. 2, pp. 2351-2366, 2019.

[14] P. Wang, H. Zhang, and V.M. Patel, "SAR Image Despeckling Using a Convolutional Neural Network," *IEEE Signal Processing Letters*, Vol. 24, No. 12, pp. 1763-1767, 2017.

[15] P. Kokil and S. Sudharson, "Despeckling of clinical ultrasound images using deep residual learning," *Computer Methods and Programs in Biomedicine*, Vol. 194, 2020.

[16] S. Liu, Y. Wang, X. Yang, B. Lei, L. Liu, S.X. Li, D. Ni, and T. Wang, "Deep Learning in Medical Ultrasound Analysis: A Review," *Engineering*, Vol. 5, No. 2, pp. 261-275, 2019.

[17] G. Litjens, T. Kooi, B. E. Bejnordi, A. A. A. Setio, F. Ciompi, M. Ghafoorian, J. A. W. M. van der Laak, B. V. Ginneken, and C. I. Sánchez, "A survey on deep learning in medical image analysis," *Medical Image Analysis*, Vol. 42, pp. 60-88, 2017.

[18] V. Nair and G. E. Hinton, "Rectified linear units improve restricted Boltzmann machines," in *International Conference on Machine Learning(ICML)*, Toronto, Canada, 2010.

[19] S. Ioffe, and C. Szegedy. "Batch normalization: Accelerating deep network training by reducing internal covariate shift." In International conference on machine learning, pp. 448-456, 2015..

[20] D. Lee, S. Choi, and H. J. Kim, "Performance evaluation of image denoising developed using convolutional denoising autoencoder in chest radiography," *Nuclear Instruments and Methods in Physics Research Section A: Accelerators, Spectrometers Detectors and Associated Equipment*, Vol. 884, pp. 97-104, 2018.

[21] D. Feng, W. Wu, H. Li, and Q. Li, "Speckle Noise Removal in Ultrasound Images Using a Deep Convolutional Neural Network and a Specially Designed Loss Function," in *International Workshop on Multiscale Multimodal Medical Imaging (MMMI),* Shenzhen, China, 2019.

[22] K. Zhang, W. Zuo, Y. Chen, D. Meng, and L. Zhang, "Beyond a Gaussian Denoiser: Residual Learning of Deep CNN for Image Denoising," *IEEE Transactions on Image*

Processing, Vol. 26, No. 7, pp. 3142-3155, 2017.

[23] Q. Zhang, Q. Yuan, J. Li, Z. Yang, and X. Ma, "Learning a Dilated Residual Network for SAR Image Despeckling," *Remote sensing*, Vol. 10, No. 2, 2018.

[24] K. He, X. Zhang, S. Ren, and J. Sun, "Deep Residual Learning for Image Recognition," in *IEEE Conference on Computer Vision and Pattern Recognition (CVPR)*, Las Vegas, USA, 2016.

[25] C. Szegedy, W. Liu, Y. Jia, P. Sermanet, S. Reed, D. Anguelov, D. Erhan, V. Vanhoucke, and A. Rabinovich, "Going Deeper With Convolutions," in *IEEE Conference on Computer Vision and Pattern Recognition(CVPR)*, Boston, USA, 2015.

[26] O. V. Michailovich and A. Tannenbaum, "Despeckling of medical ultrasound images," *IEEE Transactions on Ultrasonics, Ferroelectrics, and Frequency Control*, Vol. 53, No. 1, pp. 64-78, 2006.

[27] T. Loupas, W. N. McDicken, and P. L. Allan, "An adaptive weighted median filter for speckle suppression in medical ultrasonic images," *IEEE Transactions on Circuits and Systems*, Vol. 36, No. 1, pp. 129-135, 1989.

[28] P. Coupe, P. Hellier, C. Kervrann, and C. Barillot, "Non-local means-based speckle filtering for ultrasound images," *IEEE Transactions on Image Processing*, Vol. 18, No. 10, pp. 2221-2229, 2009.

[29] X. Hao, S. Gao, C. Kervrann, and X. Gao, "A novel multiscale nonlinear thresholding method for ultrasonic speckle suppressing," *IEEE Transactions on Medical Imaging*, Vol. 18, No. 9, pp. 787-794, 1999.

[30] A. Khvostikov, A. Krylov, J. Kamalov, and A. Megroyan, "Ultrasound despeckling by anisotropic diffusion and total variation methods for liver fibrosis diagnostics," *Signal Processing: Image Communication*, Vol. 59, pp. 3-11, 2017.

[31] A. Sawatzky, D. Tenbrinck, and X. Jiang, "A Variational Framework for Region-Based Segmentation Incorporating Physical Noise Models," *Journal of Mathematical Imaging and Vision*, Vol. 47, No. 3, pp. 179-209, 2013.

[32] J. Park, J. B. Kang, J. H. Chang, and Y. Yoo, "Speckle reduction techniques in medical ultrasound imaging," *Biomedical Engineering Letters*, Vol. 4, pp. 32-40, 2014.

[33] L. Gondara, "Medical Image Denoising Using Convolutional Denoising Autoencoders," in *International Conference on Data Mining Workshops (ICDMW),* Barcelona, Spain, 2016.

[34] W. Jifara, F. Jiang, S. Rho, M. Cheng, and S. Liu, "Medical image denoising using convolutional neural network: a residual learning approach," *The Journal of Supercomputing*, Vol. 75, No. 2, pp. 704-718, 2019.

[35] A. Coates, H. Lee, and A. Y. NG, "An Analysis of Single-Layer Networks in Unsupervised Feature Learning," in *International Conference on Artificial Intelligence and Statistics(AISTATS)*, FL, USA, 2011.

[36] T. Joel and R. Sivakumar, "An extensive review on Despeckling of medical ultrasound images using various transformation techniques," *Applied Acoustics*, Vol. 138, pp. 18-27, 2018.

[37] D. P. Kingma and J. L. Ba, "Adam: A Method for Stochastic Optimization," arXiv preprint arXiv:1412.6980, 2014.

[38] R. Kaur, M. Juneja, and A. K. Mandal, "A comprehensive review of denoising techniques for abdominal CT images," *Multimedia Tools and Applications*, Vol. 77, No. 17, pp. 22735-22770, 2018.

[39] Z. Wang, A. C. Bovik, H. R. Sheikh, and E. P. Simoncelli, "Image quality assessment: from error visibility to structural similarity," *IEEE Transactions on Image Processing*, Vol. 13, No. 4, pp. 600-612, 2004.

O. Mahmoudi Mehr was born in Nowshahr, Iran, in 1991. He obtained the B.Sc. degree in Software Engineering from University of Mazandaran, Babolsar, Iran, in 2013. He received his M.Sc. in Artificial Intelligence in 2020 from Iran University of Science and Technology, Tehran, Iran. His research interests include image processing, machine and deep learning.

M. R. Mohammadi was born in Qom, Iran, in 1987. He received the B.Sc. and M.Sc. degrees in Electrical Engineering from Amirkabir University of Technology, Tehran, Iran, in 2009 and 2011, and the Ph.D. degree in Electrical Engineering from Sharif University of Technology, Tehran, Iran, in 2015. He has been with the Faculty of Computer Engineering, Iran University of Science and Technology since 2018, where he is currently a tenured Assistance Professor. His research interests include computer vision, machine learning, and deep learning.

M. Soryani received his B.Sc. in Electronics Engineering in 1981 from Iran University of science and Technology, Tehran, Iran. He carried out his postgraduate studies at Heroit-Watt University, Edinburgh, UK, where he received his M.Sc. and Ph.D. degrees in Digital Techniques and Image Processing in 1986 and 1990 respectively. Currently he is Associate Professor in the School of Computer Engineering, Iran University of Science and Technology. His research interests include image processing, computer vision, remote sensing and medical image analysis.